Pulsed flows at the high-altitude cusp poleward boundary, and associated ionospheric convection and particle signatures, during a Cluster - FAST - SuperDARN - Søndrestrøm conjunction under a southwest IMF

C. J. Farrugia[1], E. J. Lund[1], P. E. Sandholt[2], J. A. Wild[3], S. W. H. Cowley[3], A. Balogh[4], C. Mouikis[1], E. Möbius[1], M. W. Dunlop[5], J.-M. Bosqued[6], C. W. Carlson[7], G. K. Parks[7], J.-C. Cerisier[8], J. D. Kelly[9], J.-A. Sauvaud[6], and H. Rème[6]

[1]Space Science Center and Department of Physics, University of New Hampshire, NH, USA
[2]Department of Physics, University of Oslo, Oslo, Norway
[3]Department of Physics and Astronomy, University of Leicester, Leicester, UK
[4]Blackett Laboratory, Imperial College, London, UK
[5]Rutherford-Appleton Laboratory, Didcot, Oxford, UK
[6]Centre d'Etude des Rayonnements Spatiales, Toulouse, France
[7]Space Sciences Laboratory, University of California, Berkeley, CA, USA
[8]CETP, St-Maur, France
[9]SRI International, Menlo Park, CA, USA

Abstract. Particle and magnetic field observations during a magnetic conjunction Cluster 1-FAST-Søndrestrøm within the field of view of SuperDARN radars on 21 January 2001 allow us to draw a detailed, comprehensive and self-consistent picture at three heights of signatures associated with transient reconnection under a steady south-westerly IMF (clock angle ≈130°). Cluster 1 was outbound through the high altitude ($\sim$12R_E) exterior northern cusp tailward of the bifurcation line (geomagnetic $B_x > 0$) when a solar wind dynamic pressure release shifted the spacecraft into a boundary layer downstream of the cusp. The centerpiece of the investigation is a series of flow bursts observed there by the spacecraft, which were accompanied by strong field perturbations and tailward flow deflections. Analysis shows these to be Alfvén waves. We interpret these flow events as being due to a sequence of reconnected flux tubes, with field-aligned currents in the associated Alfvén waves carrying stresses to the underlying ionosphere, a view strengthened by the other observations. At the magnetic footprint of the region of Cluster flow bursts, FAST observed an ion energy-latitude disperison of the stepped cusp type, with individual cusp ion steps corresponding to individual flow bursts. Simultaneously, the SuperDARN Stokkseyri radar observed very strong poleward-moving radar auroral forms (PMRAFs) which were conjugate to the flow bursts at Cluster. FAST was traversing these PMRAFs when it observed the cusp ion steps. The Søndrestrøm radar observed pulsed ionospheric flows (PIFs) just poleward of the convection reversal boundary. As at Cluster, the flow was eastward (tailward), implying a coherent eastward (tailward) motion of the hypothesized open flux tubes. The joint Søndrestrøm and FAST observations indicate that the open/closed field line boundary was equatorward of the convection reversal boundary by $\sim$2°. The unprecedented accuracy of the conjunction argues strongly for the validity of the interpretation of the various signatures as resulting from transient reconnection. In particular, the cusp ion steps arise on this pass from this origin, in consonance with the original pulsating cusp model. The observations point to the need of extending current ideas on the response of the ionosphere to transient reconnection. Specifically, it argues in favor of re-establishing the high-latitude boundary layer downstream of the cusp as an active site of momentum transfer.

Key words. Magnetospheric physics (current systems; magnetosphere-ionosphere interactions; solar wind-magnetosphere interactions)

---

1 Introduction

The outer magnetosphere is electromagnetically coupled to the underlying ionosphere by field-aligned currents which transmit stresses imposed at high altitudes to the ionosphere. Understanding the intricacies of solar wind-magnetosphere-

---

ionosphere interactions is a task of formidable complexity. Among the complicating factors are (i) a possible similarity of response elicited by different interplanetary triggers; (ii) the general nonlinear response of the magnetosphere to interplanetary triggers, including the possibility of saturation of response; (iii) feedback from the ionosphere; (iv) the temporal overlap of two interplanetary signals, which may re-enforce or cancel each other; (v) nonsynchronous responses of components of the coupled magnetosphere-ionosphere system to the same interplanetary trigger due to, for example, different intrinsic response times, and, most important, (vi) uncertainties in the location on the magnetopause where processes of momentum transfer, whose signatures are observed in the inner magnetosphere, are initiated.

In particular, processes of momentum and energy transfer at the magnetopause during transient reconnection of the interplanetary magnetic field (IMF) and the geomagnetic field (so called flux transfer events, FTEs, Russell and Elphic, 1978) are believed to lead to a plethora of inner magnetospheric and ionospheric signatures, the understanding of which has been an ongoing concern for over 2 decades. Individual signatures include: poleward-moving auroral forms (PMAFs; Sandholt et al., 1986, 1990, 2003), pulsed ionospheric flows/flow channels (PIFs; Pinnock et al., 1993, 1995; Rodger and Pinnock, 1997; Neudegg et al., 1999; Provan et al., 2002), poleward-moving radar auroral forms (PMRAFs; Wild et al., 2001), an ion energy-latitude dispersion signature in the cusp of the staircase variety ("stepped cusp"; Cowley et al., 1991; Newell et al., 1989; Escoubet et al., 1992). The reliable and unique association of these signatures to transient reconnection requires in general multi-point observations. By probing the signatures of coupling at various heights along the same bundle of magnetic field lines with a complement of instruments, and by interrelating the observations, magnetic conjunctions offer one of the most promising approaches to uniquely pinning down cause and effect.

A major issue which features increasingly in current debates on solar wind-magnetosphere coupling concerns the location where reconnection takes place (interconnection geometry). Specifically, in the case of transient reconnection, early evidence for its occurrence came from space probes crossing the magnetopause in two different latitude ranges: HEOS 2 at higher, and the ISEE 1 and 2 satellite pair at lower, latitudes. At higher latitudes, HEOS 2 detected short-lived ($\sim$1 min), large-amplitude fluctuations of the geomagnetic field, which were termed flux erosion events and attributed to temporarily-varying reconnection in the cusp region (Haerendel et al., 1978). Haerendel et al. found no reason to exclude the higher latitude regions as active sites of momentum transfer. Almost simultaneously, the ISEE 1/2 spacecraft detected characteristic magnetic field signatures during magnetopause crossings at lower latitudes, later associated with distinct plasma behavior (Paschmann et al., 1982; see also review by Farrugia et al., 1988). The magnetic field signature consisted primarily of a bipolar excursion of the magnetic field component perpendicular to the notional

magnetopause boundary accompanied by deflections in the field components in the local tangent plane to the magnetopause. These signatures were interpreted by Russell and Elphic (1978) as being due to reconnected flux tubes moving along the magnetopause away from the reconnection site. Later analyses confirmed this interpretation. By casting the HEOS 2 data in the same coordinate system as that used in the ISEE 1/2 analyses ("boundary normal coordinates", Russell and Elphic, 1978), Rijnbeek and Cowley (1984) established conclusively the identity of the two phenomena.

Later analyses emphasized the ISEE data set, partly because of its extensive size and superior temporal resolution and partly because of the lack of in situ observations from high magnetopause latitudes (being remedied only recently by Polar and Interball-tail). Theory thus focussed on signatures of reconnection during a southward oriented IMF initiated in the subsolar region at an X-line, which may be tilted by IMF B_y. Much progress was achieved by these means. In the meantime, however, the importance of the high-latitude boundary as a possible site of momentum transfer receded from view.

This paper concerns a multiple magnetic conjunction occurring under a southwesterly IMF where the higher altitude probe lies in a high-latitude boundary layer (HBL) poleward of the cusp. This is a location similar to that where flux erosion events were first observed, although at somewhat higher latitudes. This example was chosen because of two favourable circumstances: the location of Cluster downstream of the cusp and the possibility offered by the multiple conjunction of correlating observations there with observations at two heights in the ionosphere.

The HBL tailward of the cusp, permeated by open magnetic field lines that are stretched by the solar wind flow, is widely considered to be the site of the solar wind-magnetosphere dynamo and thus an important locale for momentum transfer to the polar cap ionosphere (e.g. Siscoe and Cummings, 1969; Vasyliunas et al., 1982; Stern, 1984; Taguchi et al., 1993; Siscoe et al., 1991; Farrugia et al., 2003). However, the role of this region as a site of momentum transfer in association with pulsed magnetopause reconnection/FTEs has not been discussed much in the literature, mainly for reasons discussed above. In this paper we report in situ plasma and magnetic field observations from the Cluster 1 spacecraft in the HBL and relate these observations to local and global plasma convection data observed simultaneously at the magnetic conjugate point in the upper atmosphere by the Søndrestrøm radar and the Iceland West (Stokkseyri) SuperDARN radar. The latter observations are characterized by PIFs and PMRAFs. These observations are in our case complemented by particle precipitation and field-aligned current data obtained from the FAST satellite. A sequence of events characterized by enhanced tailward flows are observed by Cluster 1 as the reconnected flux tubes convect past the spacecraft. These events are accompanied by Alfvénic fluctuations which, by allowing field-aligned currents to flow to the ionosphere, mediate the coupling (see, e.g. the review by Cowley, 2000). This paper thus employs

particle precipitation, magnetic field, and plasma convection data acquired at three heights in a multiple conjunction. Several hypothesized individual signatures of transient reconnection are encountered and, by discussing them within a common context, a detailed and coherent picture of the response of the magnetosphere-ionosphere system to transient reconnection emerges.

The wider implication of the investigation is that it reopens the question of the high-latitude regions as active sites of momentum transfer and, by implication, the need to extend theory to include this feature and the complex interconnection geometry suggested by the observations. The observations show, namely, that under a southwest IMF momentum transfer is taking place at the HBL/cusp poleward boundary. While the paper does not propose answers to this difficult question, it does highlight the power of magnetic conjunctions to probe the dynamics of magnetosphere-ionosphere coupling and to sharpen the points where more understanding is required. In particular, in the present case it suggests that the pulsed ionospheric flows at the cusp poleward boundary and at polar cap latitudes are excited by dynamo action taking place in the HBL. Our data sets highlight the physics of this coupling channel, where continued transfer of stress past the cusp B_x reversal point takes place. Of particular relevance for understanding the momentum coupling from the HBL is the documentation of the associated IMF B_y-regulated field-aligned current system. In our case ($B_y < 0$) this system of currents, which we call C1-C2, is located at the postnoon-dusk side boundary of the polar cap. For $B_y > 0$ conditions, the corresponding FAC pair is located on the prenoon side (Taguchi et al., 1993; Farrugia et al., 2003). The IMF B_Y-regulated dawn-dusk asymmetry of the ionospheric convection channel which is coupled to the HBL gives rise to a DPY mode of ground magnetic deflection (Svalgaard-Mansurov effect).

2   Observations

This study is based on the following data sets: interplanetary plasma and magnetic field observations from SOHO/CELIAS (Hovestadt et al., 1995) and ACE/MAG (Smith et al., 1998), supported by magnetic field measurements from Geotail (Kokubun et al., 1994); particle and magnetic field data from Cluster 1 ("Rumba") CIS (Rème et al., 1997) and FGM (Balogh et al., 1997); particle precipitation data (Carlson et al, 2001) and magnetic field (Elphic et al., 2001) from FAST; local radar measurements of plasma convection from the Søndrestrøm radar; and global patterns of ionospheric convection from the SuperDARN HF radars (Greenwald et al., 1995).

2.1   Interplanetary observations

Figure 1 shows interplanetary data from the SOHO/CELIAS and from the ACE/MAG instruments for the time interval 13:00–17:00 UT, 21 January 2001. (No ACE plasma data
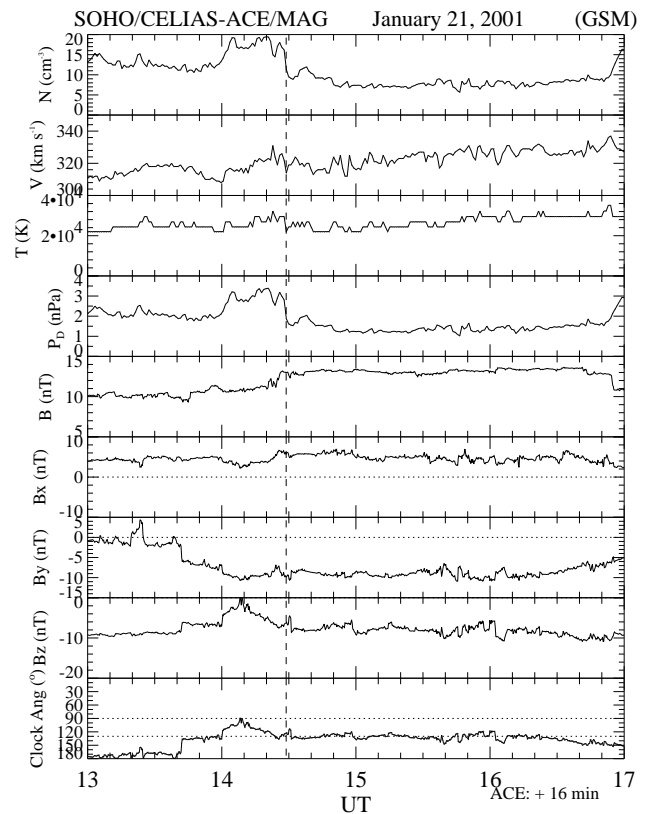
Fig. 1. Interplanetary magnetic field and plasma data from the ACE and SOHO spacecraft, respectively. The ACE data have been shifted by 16 min to account for the propagation delay from ACE to SOHO. The panels display from top to bottom, the proton number density, bulk speed, temperature, and dynamic pressure, the total field stength, GSM components of the magnetic field and the IMF clock angle. The dashed vertical guideline marks the time of a sharp dynamic pressure decrease which caused Cluster to move from the exterior cusp to the cusp boundary layer.

are available for this time period.) The time resolutions are 1 min (SOHO/CELIAS) and 15 s (ACE/MAG), respectively. From top to bottom, the panels display the proton density, bulk speed and temperature, the dynamic pressure, the total magnetic field and its components in GSM coordinates; and the IMF clock angle (i.e. the polar angle in the GSM YZ plane). ACE was located at (242.5, –1.7, 22.4) R_e (GSE coordinates), and SOHO was at (194.2, –23.0, 16.4) R_e (also GSE), both spacecraft moving little during this interval. Using a convection delay time of 16 min from ACE to SOHO, the ACE measurements have been shifted forward by this amount and plotted together with SOHO/CELIAS measurements. After the field and flow discontinuities at ~13:40 UT and 14:00 UT, the IMF is a steady, sunward-tilted field ($B_x > 0$) with strong westward ($B_y < 0$) and southward ($B_z < 0$) components. From 14:30–16:30 UT, $B_x \approx 5$ nT, $B_y \approx -10$ nT, $B_z \approx -8$ nT, and $B \approx 13$ nT, and the clock angle ~130° (second horizontal line in bottom panel). A feature which stands out clearly is the increase in dynamic pressure, P_D (due to an increase in density) to values ~3.4 nPa,
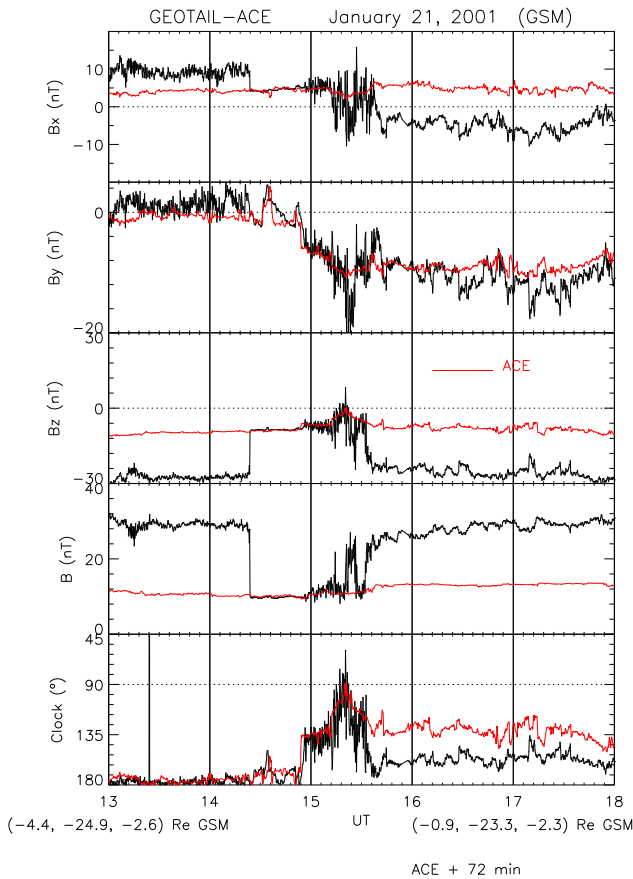
Fig. 2. An overlay of ACE (red trace) and Geotail magnetic field data. Geotail's positions at the start and end times are given at the bottom. Geotail is alternately in the solar wind (when the two traces agree) and the magnetosheath. The excellent agreement in the (i) clock angle and (ii) B_y at around 14:30–15:00 UT implies that the delay of 72 min used in the overlay is reliable.

starting at 14:00 UT at the second discontinuity and terminating at 14:30 UT. After the pressure release, this quantity remains steady at slightly lower-than-normal values of 1.5 nPa. We now wish to obtain the delay time for the interplanetary measurements at the position of SOHO to affect Cluster 1. We align the end of the pressure drop at SOHO with a strong and sharp decrease in density (from ~40 to ~10 cm^{-3}) seen on Cluster 1 (shown in Fig. 5 below). As explained when discussing the Cluster observations, this pressure drop caused the spacecraft to transit from the exterior cusp (i.e. the magnetosheath outside the cusp region), characterized by a high plasma density and low magetic field strength, to a cusp boundary layer on the poleward side of the cusp. This timing procedure yields a delay time of 68 min. To further check that this delay is correct, we compared ACE with Geotail data. Geotail was located near the dawn terminator sampling mainly the magnetosheath but crossing the bow shock occasionally. Its position was (−4, −24, 4) R_e at 13:00 UT and (−1.6, −23, 4) R_e at 17:00 UT. Figure 2 overplots the magnetic quantities from the two spacecraft (ACE in red) with a 72 min time delay included. (The Geotail data
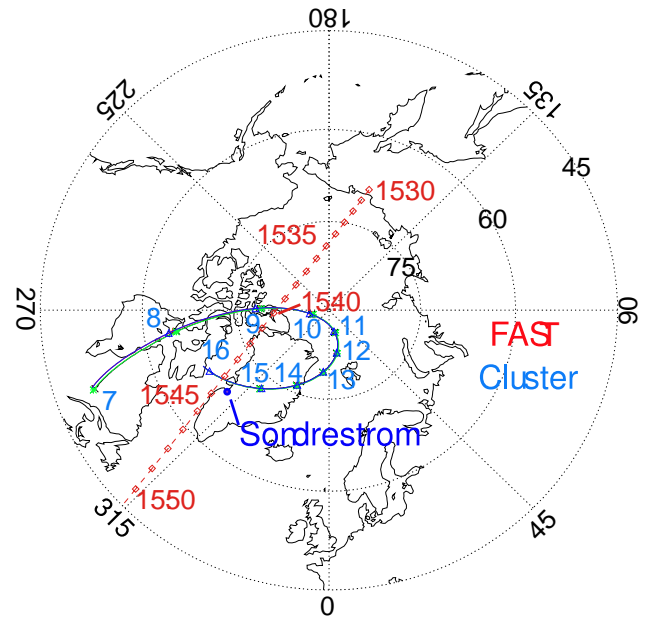

Fig. 3. An overview of the conjunction geometry in a polar geographic grid. The FAST trajectory from 15:30–15:50 UT is shown by red symbols at 1-min spacing. The green trace shows the Cluster 1 footprint for the longer time interval 07:00–16:00 UT. We shall focus on the interval 15:30–16:00 UT, where a conjunction of FAST and Cluster occured over the skies of radar station Søndrestrøm (blue dot) and in the field of view of the SuperDARN radar Iceland West.

have a time resolution of 12 s.) The agreement is very good. For example, compare quantities B_y and the clock angles between 14:24 and 15:00 UT when both spacecraft are situated in solar wind, and the clock angle profiles (panel 4), when Geotail is in the magnetosheath. Thus, given that Geotail is near the dawn terminator, while Cluster 1 is at the frontside, the 68 min SOHO/ACE-Cluster delay is reasonable.

2.2 Conjunction geometry

Figures 3 and 4 show an overview of the conjunction geometry. Figure 3 plots on a geographic grid the magnetic footprints of FAST and Cluster 1. The dotted circles refer to geographic latitudes of 45°, 60°, and 75°. The magnetic footprints of the spacecraft at an altitude of 100 km were obtained from the field line mapping of Tsyganenko's [1989] model for a Kp value=4, which is the value measured during 15:00–18:00 UT. The red symbols at 1 min spacing mark the mapped FAST trajectory from 15:30 to 15:50 UT. The magnetic footprints of the Cluster spacecraft are shown by overlapped colored traces (green: Cluster 1) for the longer time interval 07:00 to 16:00 UT for clarity. We shall examine mainly data returned by the spacecraft during 15:30–16:00 UT. At the time of nominal conjunction between Cluster and FAST, 15:44–15:45 UT, the footprints are close to the Søndrestrøm radar station in Greenland, shown by the blue dot. It can be seen that the conjunction between these three observation sites is very good.
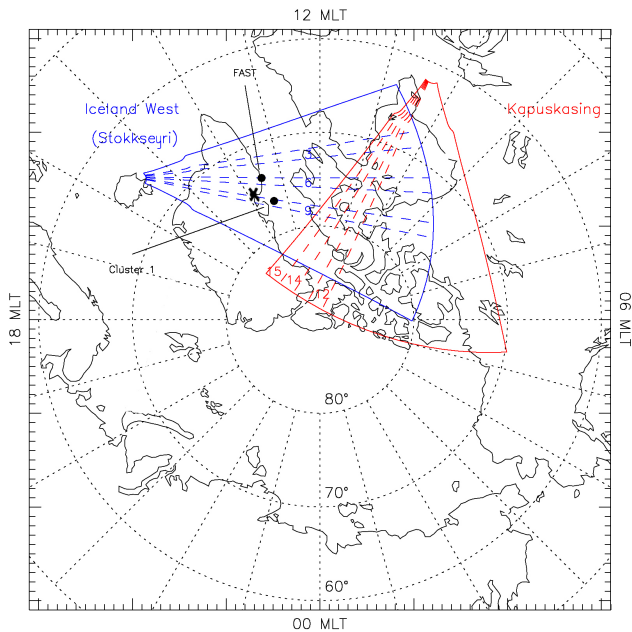
Fig. 4. The fields of view of two SuperDARN radars (Iceland West (violet) and Kapuskasing (red) in an MLAT-MLT format. The map refers to 15:45 UT, the center of the conjunction interval. Also shown are the footprints of FAST and Cluster 1 and the location of the Søndrestrøm radar station.

Fig. 5. Cluster/FGM and CIS data for 13:00–18:00 UT. Plotted are the magnetic field components in GSM coordinates and total field, the proton plasma density, temperature, flow components and total flow speed. The density panel shows the solar wind density (red) and dynamic pressure (violet), properly time-shifted. The main interval of study (15:36–16:00 UT) is shown between vertical guidelines.

To include the ground perspective, Fig. 4 shows the fields-of-view (FOV) of the SuperDARN radars at Stokkseyri (Iceland West) and Kapuskasing (in red) at 14:45 UT. Magnetic local time (MLT) is plotted against magnetic latitude (MLAT). Beams 3, 6, 9 of the Iceland West radar and beams 12, 14, 15 of Kapuskasing are indicated. The Iceland West radar FOV looks in a dusk-dawn direction across local magnetic noon. The Kapuskasing FOV looks duskward and in a much more poleward direction. Superposed on the plot are the footprints (at 15:45 UT) of FAST and Cluster 1, as mapped by Tsyganenko's 1989 model, and the location of Søndrestrøm (plus symbol). It can be seen that the footprints of FAST and Cluster 1 lie well within the FOV of Iceland West and we shall concentrate on return echoes from this radar, coordinating these with the returns for the Søndrestrøm radar.

We next describe the measurements made at the individual observing sites. In the discussion we interrelate these measurements to arrive at a comprehensive and coherent picture of solar wind-magnetosphere-ionosphere coupling during Cluster 1's sojourn in a boundary layer downstream of the cusp.
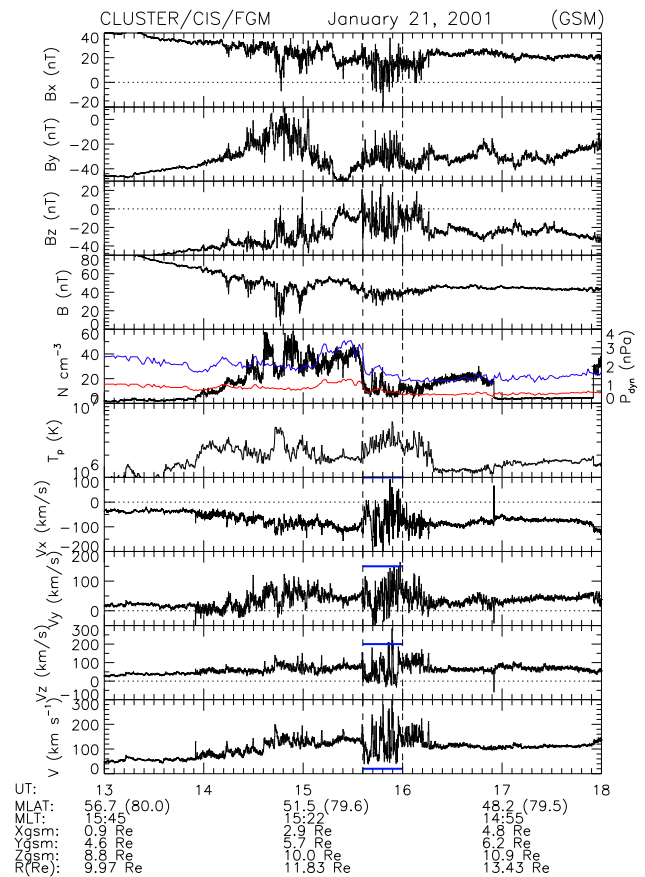
2.3 Cluster 1 observations

Figure 5 shows the magnetic field and plasma flow parameters from the Cluster 1/CIS and FGM instruments. The data are plotted at spin-average time resolution (4 s). Specifically, for the interval 13:00–18:00 UT, the figure displays the GSM components of the magnetic field, the total field, the proton density, temperature, GSM components of the flow velocity and the total bulk speed. (The drop in the density at 17:00–18:00 UT is an artefact.) The red and green traces in panel 5 are the solar wind density and dynamic pressure, respectively, time shifted as explained earlier and included for reference. Position information is given at the bottom: the UT, MLAT (invariant latitude, ILAT, in parenthesis) and MLT of the spacecraft position, its location in GSM coordinates and its radial distance. During these 5 h, the spacecraft is following an outbound orbit close to the 15:00 MLT meridian, at a radial distance which increases from 10.0 R_e to 13.4 R_e. The approximate constancy of ILAT indicates a trajectory approximately along the dipolar field L-shell at 80° ILAT.
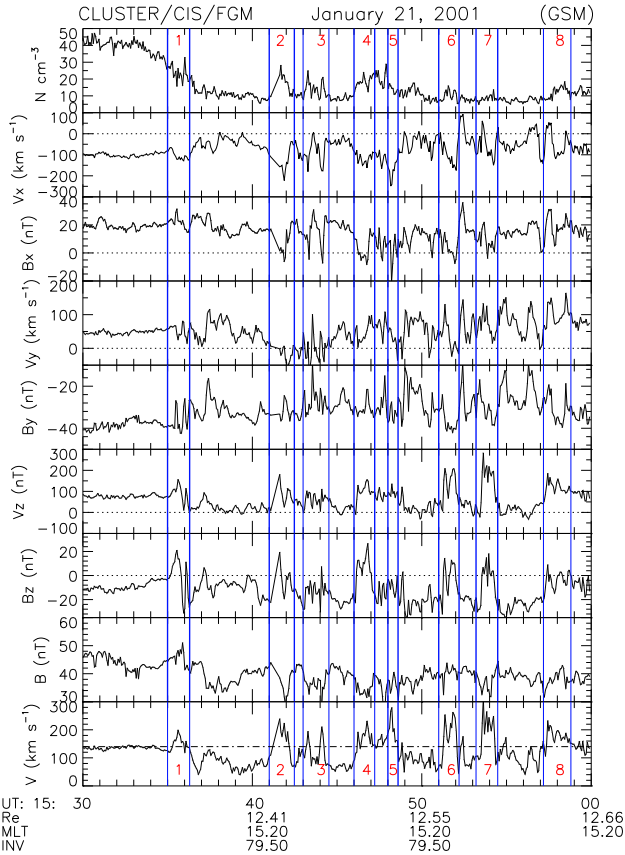
Fig. 6. An expanded view of the Cluster 1 observations during 15:30–16:00 UT. From top to bottom are displayed the plasma density, pairwise flow and field components, total field and total flow strengths. We marked and numbered all flow bursts exceeding 140 km/s (see bottom panel). The legend gives the radial distance, MLT and invariant latitude of the spacecraft.

Very low values of the density and a fluctuation-free magnetic field indicate that the spacecraft is inside the magnetosphere until ∼14:10 UT. From 14:10 to 15:30 UT, the high density and sporadically depressed field indicate a traversal through the exterior cusp. The positive B_x indicates further that the spacecraft is tailward of the bifurcation line in the Earth's magnetic field. A reorientation of the field during the passage of the high pressure solar wind takes place during 15:20–15:30 UT, where $B_z \sim 0$ and the field is mainly in B_x (>0) and B_y. This is possibly an encounter with the northern tail lobe. At 15:35 UT when the solar wind dynamic pressure decrease occurs, and for the subsequent 25 min, Cluster 1 encounters a region of plasma characterized by bursts of high speed flow (horizontal blue bars). Simultaneous with these sporadically enhanced flows, the magnetic field executes large-amplitude fluctuations. The positive GSM B_x and $B_z \approx 0$ strongly suggest that Cluster 1 is now situated in a boundary layer downsteam of the cusp. After ∼16:16 UT, the spacecraft enters the magnetosheath.

To sum up, we have an outbound pass by Cluster 1 into the high-latitude, exterior cusp at ∼12 R_E, characterized by

high density and a depressed field, and then in the boundary layer tailward of the cusp after the pressure drop arriving at 15:35 UT. A steady southwest IMF orientation was retained after the pressure change (Fig. 1). Flow bursts are seen during 15:35–16:00 UT. The phenomena associated with these flows form the centerpiece of the present multiple conjunction study.

Figure 6 shows an expanded plot of the plasma and field parameters from Cluster 1 for the interval of interest 15:30–16:00 UT: proton density, pairwise components of the flow and field, the total field and the total bulk speed. About eight flow bursts may be seen exceeding the background value of 140 km/s^{-1} (dot-dashed line, lowest panel), numbered as shown. Each flow burst is accompanied by deflections in the velocity and magnetic field components. These disturbances are particularly strong in the v_x (negative) and v_z (positive) components, indicating that the flow is deflected tailward and northward during these bursts. Note the general tendency for the density to increase within the events. This suggests a connection to the dense magnetosheath plasma. Many flow bursts are associated with strong field depressions. However, the sum of the proton and field pressures, $nkT + B^2/8\pi$, maximizes or stays nearly constant in each event (not shown).

The first flow burst is encountered shortly after the inferred entry of Cluster 1 into the cusp boundary layer. As Fig. 5 also confirms, no flow bursts were seen before this time when Cluster 1 was in the exterior cusp. This implies that under the prevailing south-westerly IMF orientation, the flow bursts are being observed only at the poleward side of the cusp.

We now consider the ensemble of flows in 15:35–16:00 UT, assume temperature isotropy of the plasma to simplify the calculations, and check the Alfvén relation:

$$\Delta\mathbf{B} = (4\pi\rho)^{1/2}\Delta\mathbf{V},$$

(see, e.g. Sonnerup et al., 1981). To obtain the perturbations in the velocity and magnetic fields we subtract the background fields by carrying out a running boxcar average of width 2 min (30 points). We then obtain the following regression lines: $\Delta B_x = 0.126 + 0.79\Delta A_x$; $\Delta B_y = -0.073 + 0.81\Delta A_y$; and $\Delta B_z = -0.063 + 1.30\Delta A_z$. The regression lines are plotted in Fig. 7, where the abscissa is $\Delta\mathbf{A} \equiv (4\pi\rho)^{1/2}\Delta\mathbf{V}$. The correlation coeffcients are 0.82 (x), 0.65 (y) and 0.86 (z) over 383 data points, which makes for a correlation valid above the 99% confidence level. We conclude that these are most likely Alfvénic fluctuations at the poleward side of the cusp. They are the Alfvénic waves which carry field-aligned current to the ionosphere, and thus mediate momentum transfer along open field lines which are generated by time-varying reconnection (Cowley et al., 1991; Glassmeier and Stellmacher, 1996; see also review by Cowley, 1999). We have thus shown directly the mediator of the MI coupling in transient reconnection in this case.

Flow bursts are concentrated in 8 or so "events", where V reaches almost solar wind values. We shall argue later, after comparison with ground-based observations and with previous studies, that these are reconnected flux tubes being
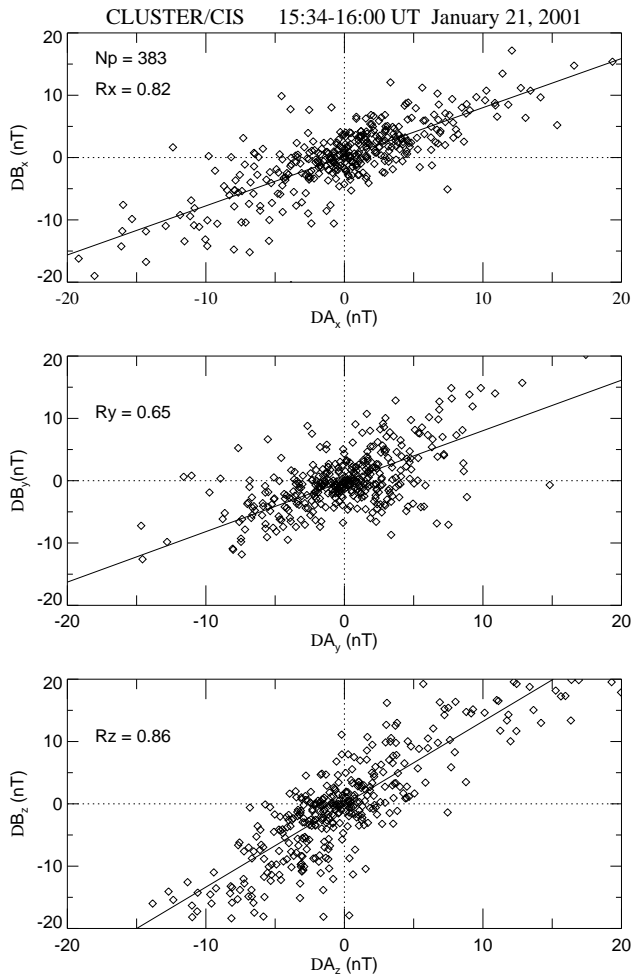
Fig. 7. The relation between the field and flow disturbances. A line of unit gradient passing through the origin would indicate perfect agreement with the Alfvénic relation under the simplification of a proton plasma and temperature isotropy. Approximate agreement with this is registered in all components. The correlation coefficients are shown in each panel.

Fig. 8. Spectrograms showing the differential energy fluxes from Cluster 1 in three pitch angle bins, from top to bottom, along (pitch angle between 0 and 30°), perpendicular (80–100°) and antiparallel to the magnetic field (150–180°). The flow burst times are shown by vertical guidelines. The data are consistent with the concept of tailward–convecting flux tubes passing over Cluster.

swept past Cluster. They are being observed at a boundary layer downstream of the cusp, when their motion is governed mainly by the magnetosheath flow. We recall that this location is not far from that where Haerendel et al. (1978) originally reported flux erosion events (see also Rijnbeek and Cowley, 1984), which were attributed to pulsed reconnection.

Directional information on the plasma flow may also be inferred from the spectrograms of Fig. 8, which show differential energy fluxes at Cluster 1 in three pitch-angle windows: 0–30° ("parallel" to the field), 80–100° ("perpendicular" to the field), and 150–180° ("antiparallel" to the field). It appears that during the flow bursts, the antiparallel and perpendicular components to the field are enhanced in the events. In most of the cases, therefore, there appears to be a net plasma outflow at Cluster 1, i.e. flows directed tailward.
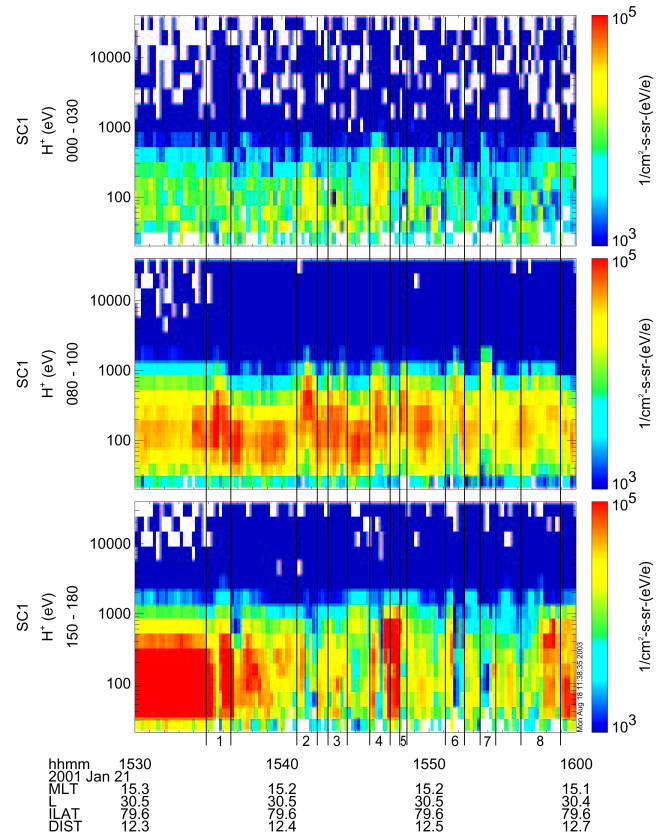
2.4 FAST observations

A confirmation that the pulsed flows at Cluster are indeed reconnection-related comes from a fortuitous quarter: FAST, making observations in the topside ionosphere conjugate to Cluster 1. Recall that nominal conjunction with Cluster 1 took place at ~15:44–15:45 UT. In the interval 15:42 and 15:47 UT, FAST was following the ~13:00 MLT meridian at an average height of about 900 km with an ILAT which decreases from 82.2° to 64.9°. In this interval it recorded an ion energy-latitude dispersion of the stepped cusp variety.

The relevant data is shown in Fig. 9 which displays electron and ion spectrograms for the period 15:42–15:47 UT. FAST is initially in the polar cap, characterized by the presence of a tenuous and homogeneous electron precipitation up to ~500 eV and the absence of ion precipitation, indicative of polar rain. Cusp/mantle precipitation is then encountered between 15:43:42 UT and 15:44:20, extending from 76.5° and 74.3° ILAT. Cusp/cleft precipitation is encountered between 15:44:20 and 15:44:40 UT. After ~15:45 UT, ion differential energy fluxes reach up to high energies, originating from the dayside extension of the central plasma sheet (CPS; Newell
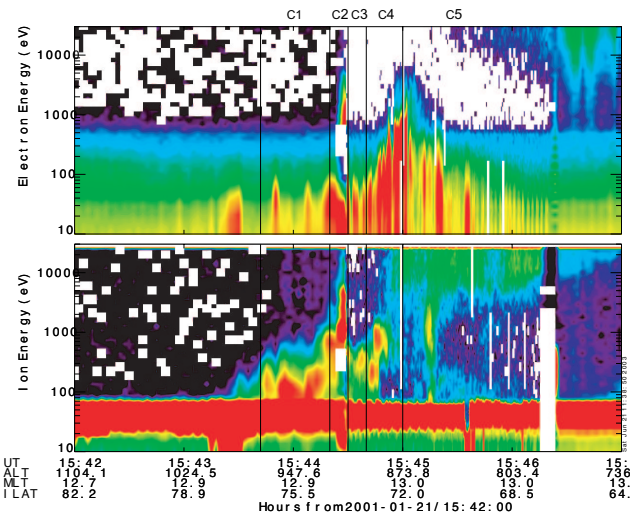
Fig. 9. Electron and ion spectrograms from FAST for the interval 15:42–15:47 UT, during which FAST descends 17.3° in ILAT, moving approximately along the 13:00 MLT meridian. Vertical lines have been drawn to delimit the extent of the field-aligned currents described in Fig. 10.
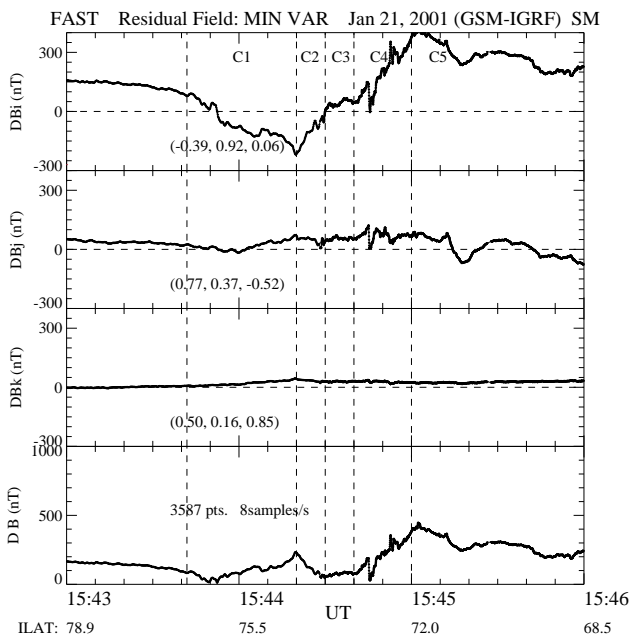

Fig. 10. The 8 sample/s magnetic field at FAST presented in minimum variance coordinates. The axes coordinates thus derived are shown in an SM system in each panel. The vertical lines bracket different currents from the different gradients in the ~east-west component (top panel): into the ionosphere when the gradient is negative; out of the ionosphere when the gradient is positive.

and Meng, 1992). Since the latter are on closed field lines, and the former are believed to be on open field lines, the open/closed field line boundary is encountered by FAST at ~15:45 UT at an ILAT of ~72°.

When inside the cusp/cleft, two subregimes are encountered which are both characterized by a mixture of cusp-type

and dayside boundary plasma sheet (BPS; Newell and Meng, 1992; Lockwood, 1997) electron precipitation. The latter electrons extend to above 1 keV. In the ion data these regimes form a three-step precipitation feature (staircase-type signature). This is a stepped cusp ion energy-latitude dispersion predicted by Cowley et al. (1991) to result from transient reconnection (see also Lockwood and Smith, 1989; Newell and Meng, 1991; Escoubet et al., 1992). The lower energy cutoff increases with decreasing latitude as the spacecraft intercepts progressively "younger" reconnected flux tubes (i.e. those which were reconnected later). In an ILAT span of about 3 deg, we can make out three cusp ion steps. Note that a 3-deg ILAT span at 900 km height maps out to a much longer distance at Cluster 1 heights, which Cluster 1 would take many minutes to traverse. We conclude therefore that the plasma flow bursts at Cluster 1 in the appropriate time interval are related to the steps in the staircase ion dispersion near 13:00 MLT. Following the interpretation of stepped cusp (e.g. Cowley et al., 1991; Lockwood and Smith, 1992, 1994), we have a self-consistency check that the flow bursts at Cluster 1 are reconnection-related.

The direction of the currents threading the stepped cusp precipitation at FAST may be inferred from the gradients in the east-west component of the magnetic field. Data are available in SM coordinates at 8 samples s^{-1} from which the IGRF 1995 model field has been subtracted. The SM coordinate system has the z-axis pointing along the Earth's dipole, the XZ plane contains the solar direction, and the y-axis is positive east. We carry out a minimum variance analysis (Sonnerup and Cahill, 1967) for the interval 15:43–15:46 UT, which contains the stepped cusp precipitation. The results are shown in Fig. 10. The routine picks out a very well-defined normal (ratio of intermediate to minimum eigenvalues = 22.6). The normal component of the field is B_k=24.8 ± 9.1 nT. The coordinates of the principal axes are noted in the different panels of Fig. 10. (The last panel DB gives the difference between the measured field and IGRF95.) In particular, DB_i is the magnetic deflection mostly along the east-west direction (y-component=0.92). The stepped cusp is threaded by a pair of currents, marked C1 and C2. The negative gradient in C1 seen by a spacecraft travelling equatorward implies a current into the ionosphere on the poleward side (down; mantle region) and the positive deflection in C2 is a current out the ionosphere on the equatorward side (up). Thus, the lower latitude part of the cusp has an upward current and the higher latitude has a downward current. This is as expected for the cusp currents for IMF B_y<0, as seen here (Cowley, 1981; Lee et al., 1985; Taguchi et al., 1993; Watanabe et al., 1996.). We shall see later that this current arrangement results in an eastward (tailward) **E** x **B** drift that is consistent with the direction of the local convection flow seen by the Søndrestrøm radar.

Combining Figs. 9 and 10 we can now describe the stepped cusp more closely. As FAST descends in latitude, it first meets the oldest reconnected flux tube, whose current (into the ionosphere) is denoted in Fig. 10 by C1. In its progression tailward, this flux tube is already in mantle precipitation,

as evidenced by the low energies. Note that the Cluster footprint lies in this regime, too, so for this work this is the most relevant cusp ion step. FAST then encounters a shorter precipitation step, separated from the first by a upward jump in the lower energy cutoff (15:44:20–15:44:23 UT). Another upward jump in energy occurs at the beginning of the third step (15:44:23–15:44:29 UT). The ion energies extend up to about 5 keV. These are denoted by C2 in Fig. 10 and are threaded by an upward flowing current. These two flux tubes are in an earlier state of evolution than the first one, and this is evidenced by the higher energy of the precipitation typical of the cusp/cleft region. FAST thus traversed a 3-stepped staircase ion dispersion as it goes from 76.5 to 73.7° ILAT.

A region intervenes (marked C3 in Fig. 10) characterized by weaker precipitation and smaller current density. After this, an apparent 2-stepped cusp precipitation is re-encountered (C4 in Figs. 9 and 10) with an upward current flowing through it. These flux tubes are marked by a higher energy electron precipitation than the former. Furthermore, the ion signature shows evidence of a double (overlapped) dispersion in the lower step (~15:44:44–15:44:50 UT). Equatorward of this cusp ion step strong electron precipitation appears in the energy range ~0.1 -1 keV. This belongs to the category of dayside BPS precipitation (see Newell and Meng, 1992; and Lockwood, 1997). C5 is characterized by a wide latitudinal range of homgeneous CPS precipitation.

2.5 SuperDARN observations

Global spatial maps of the ionospheric convection pattern generated using the map potential algorithm of Ruohoniemi and Baker (1998) are displayed in an MLAT-MLT format in Figures 11 a–c. To produce these plots, line-of-sight velocity data from 8 Northern Hemisphere SuperDARN radars were employed. Details of the algorithm parameters are shown at lower left. We used a 60-min lag time - not a critical quantity in steady IMF conditions such as these and, in any case, close to the delay time we inferred above - to select the appropriate statistical model to fill in data gaps. Excellent data coverage exists on the post-noon sector anyway, so this region is practically independent of statistics. The FAST trajectory has been overlaid on these plots. The bars on the FAST trajectory represent the latitudinal range traversed by FAST during the corresponding 1-min SuperDARN radar scan. The relation of FAST observations to the global convection is discussed later. Here we concentrate on the SuperDARN observations.

The three figures refer to the interval 15:43:00-15:46:00 UT in 1 min segments, a time span corresponding to the middle of the interval of interest. The figures show the measured ionospheric convection pattern with continuous streamlines superposed. A convection throat is apparent from 11:00–13:00 MLT. Very evident is the presence of pre- and post-noon convection cells. There is only a slight asymmetry about the noon meridian, but this may be because the eastward flows observed by Søndrestrøm in the poleward region are not well imaged by SuperDARN, so the

actual asymmetry may be underrepresented. The maps indicate that the large-scale picture of the dayside convection pattern is imaged rather well, with particularly large noonward flows (of the order of 1000 m/s^{-1}) generally centred at around ~13:00–14:00 MLT and 72–75° MLAT, the latter being the FAST position between 15:44 UT–15:45 UT (Fig. 11b). Somewhat smaller-magnitude flows, also noonward at this MLT-MLAT location, are also seen in the pre-noon sector at ~07:30–09:00 MLT and ~75° MLAT. Presumably both these flow regions are a consequence of ongoing reconnection as flux is opened and dragged into the polar cap region (Greenwald et al., 1995).

The post-noon sector flows are particularly well observed by the Iceland West radar (symbol W in Figures 11, near top left). Earlier, Fig. 4 showed the FOV and selected beams of this radar, as well as those of the Kapuskasing (symbol "K" in Fig. 11, top right) radar in an MLT/MLAT coordinate system at 15:45 UT. For the 1-hour interval 15:15–16:15 UT, Fig. 12 shows returns from the beams 3, 6, 9 (those indicated in Fig. 4) from the Iceland West radar at Stokkseyri. For each of the individual beams, the l-o-s Doppler shifted velocity and the received backscattered power are plotted. All the velocity panels have a uniform colour coding; likewise for the backscatter power panels.

The pulsed velocity structures (shown arrowed in the beam 6 panels) are very striking. In each beam, flow channels containing high l-o-s velocities (red color) can be seen moving away from the radar, this direction corresponding to a mainly westward motion (Fig. 4). This sense of motion of the structures can also be clearly seen in the backscattered power data (see, e.g. panel 4). The flow speed is remarkably high, in excess of 1500 m s^{-1} at times. These are classic examples of poleward moving radar auroral forms (PMRAFs; shown by slanted lines for those within the interval covered also by Cluster observations; Wild et al., 2001), which are the radar counterpart of the optical poleward moving auroral forms (PMAFs; Sandholt et al., 1986, 1990). In line with previous work (Wild et al., 2001, and references therein) we interpret these as the signatures of flux transfer events.

There is a close correspondence between the velocity pulses seen by Beam 6, which is close to the Cluster footprint (Fig. 4), and the flow enhancements seen by Cluster and shown in Fig. 6. This remarkable correspondence is highlighted by arrows in both the Doppler l-o-s velocities and in the backscatter power. An exact agreement between the numbers of flow bursts on Cluster and the PMRAFs is neither present nor is it expected. As explained in Neudegg et al., 2000, when FTEs at the magnetopause repeat in intervals shorter than the response time of the ionosphere, the radars are not able to resolve individual FTE signatures, but only give a general enhancement of the flow.

We have marked at the top of Fig. 12 the intervals corresponding to the FAST and Cluster 1 passes, respectively. The relationship between FAST and Cluster observations in the interval marked on the SuperDARN measurements will be taken up in the Discussion.
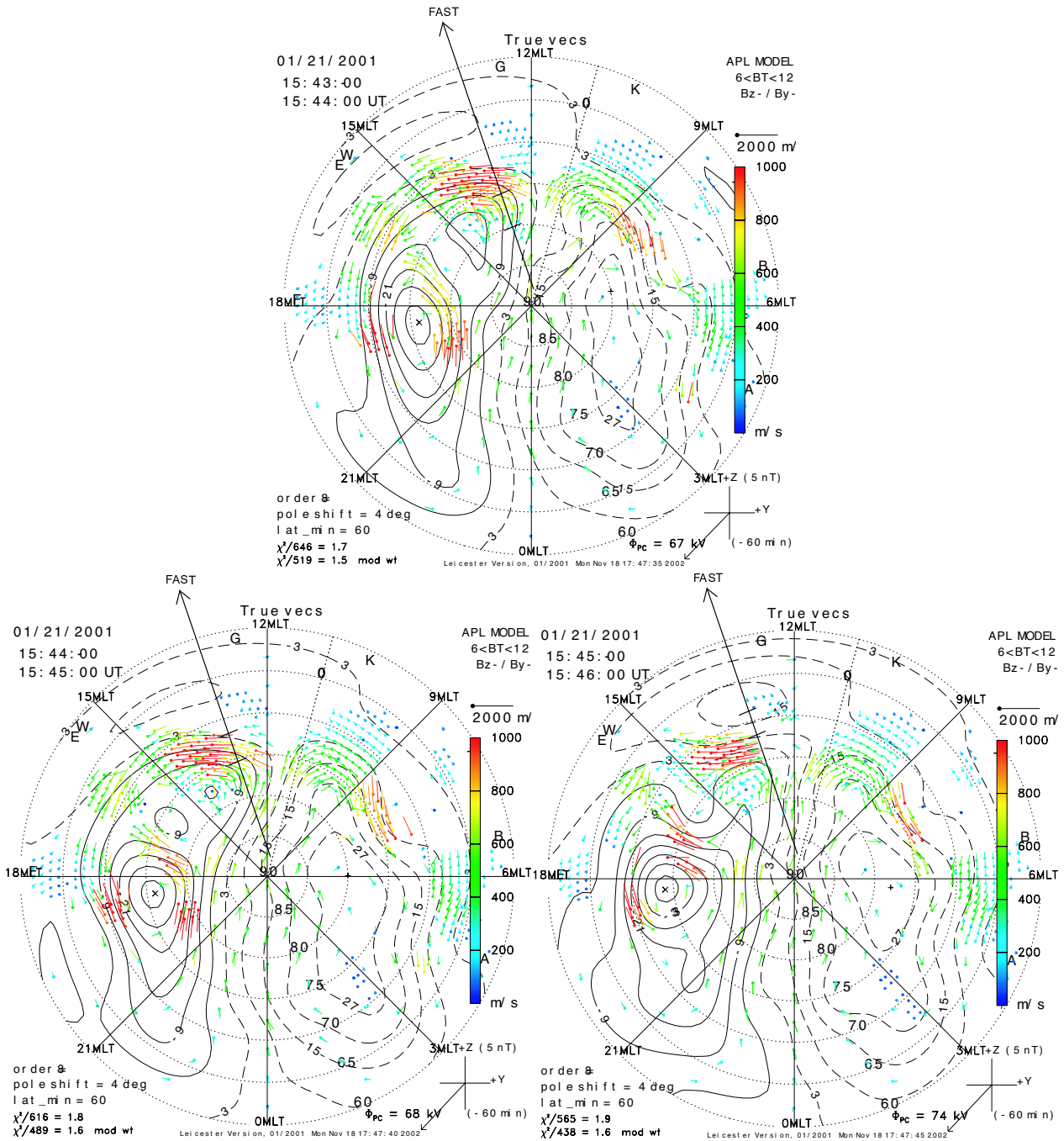
Fig. 11. (**a**) SuperDARN spatial plots giving the global convection. For further details, see text. The FAST trajectory is indicated and the segment thereof traversed during the 1-min interval shown is indicated by a bar. (**b**) Same as Fig. 11a, but for 15:44–15:45 UT. (**c**) Same as Fig. 11a, but for 15:45–15:46 UT.

2.6 Observations from the Søndrestrøm radar

We now show details of the latitudinal profile of the ionospheric flow at 13:00 MLT as obtained from the local station Søndrestrøm. Velocity vectors from this radar are plotted in a magnetic latitude versus UT format for the interval 15:30–16:00 UT in Fig. 13. One complete scan takes ∼4 min. Red coloring indicates westward- and violet indicates eastward-directed flows.

The radar documents well the position of the convection reversal boundary during the interval we study. Located initially at ∼74°, it shifts northward by 1.5 deg during the next 10–15 min and then approaches 74° again at the end of the interval. Comparing with FAST observations of the open/closed field line boundary (at 72°, Fig. 9) the convection reversal is located ∼2° poleward of this.

At the time of our conjunction, strong eastward (tailward) flows occur within 76–77° MLAT immediately poleward of the convection reversal. They reach a maximum of ~2000 m/s^{-1}. These flows are located near the footprint of Cluster 1, which also observed eastward (tailward) flows. These flow pertubations corrugate the convection reversal boundary, as predicted by Cowley et al. (1991) and Lockwood (1997). The flows at Søndrestrøm are examples of pulsed ionospheric flows which are coupled to the solar wind-magnetosphere dynamo in the HBL, along old open flux tubes that were generated at an earlier stage by a transient reconnection process (Pinnock et al., 1993, 1995; Rodger and Pinnock, 1997; Neudegg et al., 1999; Provan et al., 2002). The pulsed flows equatorward of the convection reversal (directed westward) are related to newly-opened field lines, while the channel of strong eastward flows poleward of the convection reversal is situated on older open flux coupled to the solar wind-magnetosphere dynamo in the HBL. The pulsed nature of the aurora in this MLT sector (poleward of the convection reversal) has been documented for a similar IMF condition ($B_y < 0$) by Farrugia et al. (1995).

3 Discussion

We have presented a comprehensive description at three altitudes (the high-latitude magnetopause boundary layer, the topside ionosphere at ~900 km, and the ionosphere at 200–500 km altitude, the latter referring to the altitude range of the radar range gates) of reconnection-associated enhanced flows, precipitation, ionospheric flow channels, and large-scale convection patterns, thereby uniting various strands in the current understanding of magnetosphere-ionosphere (MI) coupling during time varying reconnection. Elements of this current understanding addressed in the work were: (i) bursts of high speed flows at a boundary layer downstream of the cusp; (ii) Alfvén waves carrying field-aligned currents to the ionosphere down reconnected flux tubes; (iii) a ion energy-latitude dispersion signature of the staircase type; (iv) pulsed ionospheric flows (PIFS); and (v) poleward-moving radar auroral forms (PMRAFs). The obervations were acquired during a magnetic conjunction of Cluster 1 (outbound through the cusp poleward boundary at 12R_E), FAST (at the topside ionosphere at altitudes of 800–1000 km), and the Søndrestøm radar which took place within the FOV of the SuperDARN radar Iceland West. The observations benefitted by FAST's ability to separate spatial from temporal structures. The emphasis of this paper is on phenomenology. In this discussion we therefore relate the observations at the various heights pairwise, to establish a self-consistent picture of the response to momentum transfer at high-latitudes. Finally, we mention the importance of the observations on theories of the generation of momentum transfer during solar wind-magnetospheric-ionospheric coupling.
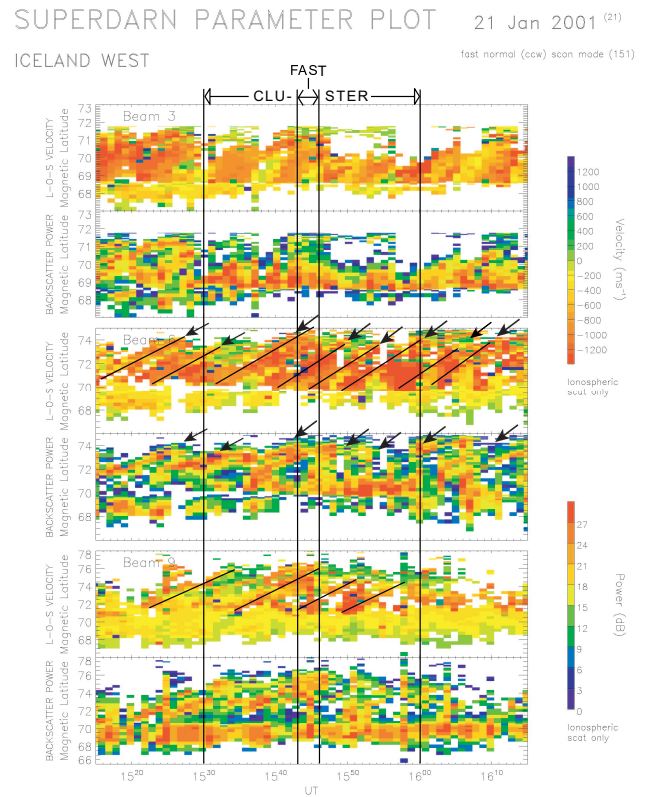

Fig. 12. Returns (l-o-s Doppler - shifted velocities and backscatter power) from beams 3, 6, and 9 of the CUTLASS/SuperDARN radar station Iceland West. The outer vertical guidelines indicate the conjunction with Cluster, while the inner, that with FAST. On beam 6 we have shown by arrows the flow bursts moving poleward, also marked by slanted lines. Flows of around 1000 m/s^{--1} and higher are observed.

3.1 Correlating the observations

3.1.1 Cluster 1 and SuperDARN

We now relate Cluster 1 and SuperDARN measurements when Cluster 1 is observing fast flows from 15:30–16:00 UT (Fig. 6). The flow at Cluster is bursty in nature, with high speed jets of the order of 220 km/s^{-1}, which is a substantial fraction of the speed of the solar wind (Fig. 1), recurring every 2–5 minutes. In Fig. 6, all flows which are above a certain background value (140 km/s) are marked, irrespective of their duration or proximity to neighboring flows. The field line mapping in Fig. 4 shows the Cluster footprint to be close to the FOV of beam 6 of the Iceland West radar, so that we compare Cluster observation with the echoes from beam 6. In the Iceland West plot of Fig. 12, this interval is delimited by the outer vertical guidelines. A sequence of poleward-moving radar auroral forms (PMRAFs/PIFs) is seen by the radar, marked by slanted lines and arrows. The lifetime of the individual PMRAFs within the FOV of the radar is 10–15 min. They recur at a rate of 1 every 4–5 min on average. It thus appears that the repetition rate is slower on SuperDARN
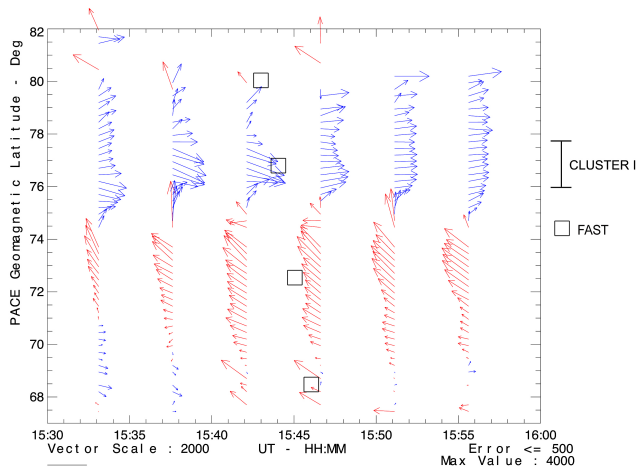
Fig. 13. Ion drift velocities from the Søndrestrøm radar between 15:30–16:00 UT. A clear convection reversal boundary may be seen between latitudinal sectors of noonward (sunward, red) and tailward flow (violet). Note the boundary corrugations. Tailward flows of the order of $2 \, \text{km/s}^{-1}$ are observed poleward of the convection reversal. These flows are being seen at the footprint of Cluster at 15:40–15:45 UT.

than on Cluster. Previous studies of repetitive ionospheric flows (Wild et al., 2001), and references therein) have, however, established that two neighbouring flow bursts will not be distinguished separately from the background and will merge if they recur within less than 2–3 min of each other. Bearing this in mind, we feel that the correspondence at the two heights is impressive. We may consider the flow bursts at Cluster 1 as the high-altitude counterpart of the PIFs at ionospheric heights.

3.1.2 Cluster 1 and Søndrestrøm

Søndrestrøm lies close to the footprint of Cluster (Fig. 3). The Cluster footprint lies inside the channel of eastward (tailward) flows recorded by the radar just poleward of the convection reversal boundary. The radar measured flow speeds reaching values of $\sim 2 \, \text{km/s}^{-1}$ (Fig. 13). In addition, the ionospheric flows are also bursty, as inferred from SuperDARN. We emphasize that the enhanced flows are also directed in an eastward (tailward) direction, i.e. in the same direction as the high speed flows at Cluster, which were of order $240 \, \text{km/s}^{-1}$. The agreement at two heights with respect to the flow direction and intermittent character furnish a strong consistency check on our interpretation of a sequence of reconnected flux tubes sweeping past Cluster, implying as it does a coherent motion of the hypothesized reconnected tubes.

3.1.3 Cluster 1 and FAST

Through the joint FAST-Cluster observations, the Cluster footprint is inferred to be embedded in the regime of mantle precipitation and associated FACs. We have produced

direct observational evidence of Alfvénic structures at Cluster. These are the waves which carry field-aligned currents to drive the ionosphere. It would be desirable to also confirm their presence at FAST. This is impracticable, however, partly because of the very disparate resolution of the field and plasma data (the former being 40 times the latter), but mainly because the density and the composition at FAST heights vary strongly with altitude and FAST does change its altitude from $\sim 1000 \, \text{km}$ to $\sim 800 \, \text{km}$ in the 2 min from 15:43:30-15:45:30.

The stepped cusp ion precipitation was observed by FAST at the ionospheric footprint of magnetic field lines at the high altitude portion of which flow bursts were observed by Cluster. This is a further consistency check that what we are witnessing at FAST is the effect of temporal changes in the reconnection rate. In previous work, Yeoman et al. (1997) and Farrugia et al. (1998) associated a stepped cusp ion precipitation with poleward moving auroral forms, the latter long held to be auroral signatures of pulsed reconnection (Sandholt et al., 1986, 1990). Here we have emphasized the flow channel that is excited at the polar cap boundary in the postnoon sector during the prevailing negative B_y conditions.

3.1.4 FAST and SuperDARN

In Figs. 11a-c, we have overlaid the mapped footprint of FAST on the global convection pattern. At 15:43–15:44 UT (Fig. 11a) FAST is just poleward of the strong noonward flows located at 13:00 MLT, and traversing a region of slightly weaker, but poleward flows. According to the FAST spectrograms of Fig. 9, in this 1-min interval FAST recorded polar rain and mantle precipitation. During 15:44–15:45 UT (Fig. 11b), i.e. during the nominal conjunction, the footprint of FAST is crossing the region of enhanced noonward and poleward flows. Correspondingly, Fig. 9 shows that the spacecraft is observing at this time, in a magnetic latitude range 73.0–76.4°, a stepped cusp, consisting of 3 cusp ion steps. According to Fig. 4, at ~15:45 UT, FAST is in the FOV of beam 6 of the SuperDARN station Iceland West. Consulting the Doppler shifted velocities of beam 6 of this radar (Fig. 12), we see that in the latitude range 72–75° the radar picks out two distinct PMRAFs in different stages of evolution, the one at lower latitudes being the "younger" (more recently reconnected). Through the conjunction, therefore, we have established a close correspondence between two individual cusp ion steps and two convection events (PMRAFs). This correspondence between the flows and the stepped cusp has, to our knowledge, never been delineated before in such detail. It is thus clear that the stepped cusp in this event arises out of a temporal phenomenon, in this case, transient reconnection. Nevertheless, this cusp appears equatorward of the flow reversal boundary.

In work by Trattner et al. (1999, 2002a, b) the case for a spatial interpretation of cusp ion steps was argued. This was based on the observation in case event studies of the same structures (stepped cusp) being seen by two spacecraft even when their cusp traversals were separated by hours. This

work of Trattner et al. shows that, sometimes, spatial structuring does occur. However, the present work demonstrates clearly that cusp ion steps can indeed be due to temporal variations in the reconnection rate, in accord with the original "pulsating cusp" model (Cowley et al., 1991; Lockwood and Smith, 1992, 1994). In recent work, it has been even possible in a case example to separate spatial from temporal features of the cusp, where the the temporal interpretation of the cusp ion steps themselves was retained (see Farrugia et al., 2004).

During 15:45–15:46 UT, (Fig. 11c), FAST is in the latitude range 72.0–68.5° and traversing the equatorward boundary of the flow convection channel. The spectrograms of Fig. 9 show at this time that FAST entered into CPS-type precipitation, hallmarked by homogeneous and energetic ion fluxes. These ion fluxes are accompanied by discrete, increased electron fluxes of energy <300 eV. At this time, FAST is in the FOV of beam 3 of the Iceland West radar, which sees a flow burst at the same latitudes (top panel of Fig. 12). This points to a correspondence between CPS precipitation and pulsed ionospheric flows, and may imply that transient reconnection has also affected the convection on closed field lines. Such a notion is consistent with the Cowley and Lockwood (1992) model of the excitation of ionospheric flows.

3.1.5 FAST and Søndrestrøm

FAST crossed into CPS precipitation on closed field lines at ∼15:45 UT when, as stated, it was in the latitude range 72.0–68.5°. The Søndrestrøm flow data confirm that this open-closed field-line boundary lies equatorward of the convection reversal boundary by about 2 degrees (Fig. 13). Note that the SuperDARN PIFs seen by Iceland West appear to have been mainly in the lower latitude region of continuing westward flow.

In the Søndrestrøm plot of Fig. 13 we have marked by open squares the position of the FAST footprint at 15:43, 15:44, 15:45, 15:46 UT. (Note that we use corrected geomagnetic latitudes computed for the year 2001 and mapped to 100 km. At the Earth's surface the PACE geomagnetic coordinates and the corrected geomagnetic coordinates are identical.) Consulting this figure and Fig. 9, we establish the following correspondencies. At 15:44 UT, the footprint is in the center of the channel of strong eastward (tailward) flows north of the convection reversal. From Fig. 9 we find that this corresponds to particle precipitation and FAC regime C1, characterized by downward FAC and mantle precipitation. We find that the channel of strong eastward (tailward) flows is electromagnetically connected with the C1-C2 field-aligned system. At 15:45 UT the footprint now lies equatorward of the convection reversal, on westward flows. From Fig. 9, this corresponds to the interface C4/C5, which is the open-closed field line boundary. Thus this boundary is located 1–2 deg south of the convection reversal. At 15:46 UT FAST is near the equatorward boundary of the channel of strong westward flows, on closed field lines. From Fig. 9, FAST is at this time well within the regime of CPS precipitation. The present observation of enhanced flow speed in the regime of mantle precipitation is consistent with PIF characteristics that were previously observed (Provan et al., 2002; Sandholt et al., 2003).

3.2 The observations in the context of solar wind-magnetosphere interactions

A broader issue on solar wind-magnetosphere-ionosphere coupling raised by the multiple conjunction concerns the role of the high-latitude boundary layer in momentum transfer under a southwest IMF. In classical theories of reconnection between the IMF and the geomagnetic field, it is often assumed that for an IMF with a strong southward component, as here, reconnection takes place at subsolar latitudes. The reconnected flux tubes formed by transient reconnection then move tailward and poleward under a combination of magnetic tension forces ($\mathbf{j} \times \mathbf{B}$) and magnetosheath flow. By the time they reach the downstream side of the cusp, the $\mathbf{j} \times \mathbf{B}$ force has reversed and the reconnected flux tubes are extracting energy from the flow (Tanaka, 2003).

At the time when flux erosion events were first seen in HEOS 2 data, at a locale comparable to ours, Haerendel et al. (1978) suggested that "entry of magnetosheath plasma should not be restricted to the cusp region but may continue further down the tail or along the early morning or late evening flanks, depending on the initial orientation of the external field. The interface with the tail probably consists of a rotational discontinuity followed by an expansion wave." The subsequent remarkable advances made through the analysis of the extensive ISEE 1 and 2 data sets, obtained at lower latitudes, shifted attention to the subsolar region as the place where FTEs - equivalent to flux erosion events, Rijnbeek and Cowley (1984) - are initiated and momentum transfer takes place. Our detailed observations suggest, however, that the original suggestion of Haerendel et al. (1978) may need to be re-assessed. In particular, the high-latitude boundary layer (HBL) may be an active site of momentum transfer from the solar wind to the magnetosphere during those events which at low altitudes are manifested in the form of high-speed flows in the regime of mantle precipitation, the PIFs.

The channel of high-speed flows is coupled to the C1-C2 FAC system. This current system is identical to the IMF B_y-regulated HCC-LCC currents of Taguchi et al. (1993). In this study we reported the version of the current system which is appropriate to the prevailing $B_y < 0$ conditions. The corresponding current system for $B_y > 0$ is located on the prenoon-dusk side of the polar cap. The association between the high-latitude plasma source, field-aligned currents and aurora for the latter case was documented by Farrugia et al. (2003) in a Polar-ground conjunction study. The IMF-regulated dawn-dusk asymmetry of this current system/ionospheric convection channel, which is coupled to the HBL, gives rise to a DPY mode of ground magnetic deflection (a Svalgaard-Mansurov effect).

In conclusion, we have addressed the issue of pulsed reconnection signatures in the coupled magnetosphere-ionosphere system using a complement of data sets in a

multiple conjunction, and emphasized the importance of the HBL as a locale where continued transfer of stress takes place. Our study was based on just one event, reserving an analysis of many events for future work. We note, however, that in a very recent work Thompson et al. (2004) observed the same type of impulsive events, though they discussed them only from the Cluster perspective. The focus there was on a sequence of reversals of the GSM B_z field component observed downstream of the cusp, each reversal being ascribed to currents flowing perpendicular to the field. These confined perpendicular currents are likely to connect with the FACs we have discussed above.

References

Balogh, A., Dunlop, M., and Cowley, S. W. H. et al.: The Cluster magnetic field investigation, Space Sci. Rev., 79, 65–91, 1997.

Carlson, C. W., McFadden, J. P., Turin, P., Curtis, D. W., and Magoncelli, A.: The electron and ion plasma experiment for FAST, Space Sci. Rev., 98, 33–66, 2001.

Cowley, S. W. H.: Magnetospheric asymmetries associated with the *Y*-component of the IMF, Planet. Space Sci., 29, 79–86, 1981.

Cowley, S. W. H.: Magnetosphere-ionosphere interactions - a tutorial review, in Magnetospheric current systems, Geophys. Mon. 118, edited by Ohtani, S., Fujii, R., Hesse, M., and Lysak, R. L., AGU, Washington, D.C., 91–106, 2000.

Cowley, S. W. H., Freeman, M. P., Lockwood, M., and Smith, M. F.: The ionospheric signature of flux transfer events, in Proceedings of the International Workshop on Cluster Dayside Polar Cusp, ESA SP-300, 105–112, 1991.

Cowley, S. W. H. and Lockwood, M.: Excitation and decay of solar wind-driven flows in the magnetosphere-ionopshere system, Ann. Geophysicae, 10, 103–115, 1992.

Cowley, S. W. H., Morelli, J. P., Freeman, M. P., Lockwood, M., and Smith, M. F.: Excitation and decay of flows in the magnetopshere-ionopshere system due to magnetic reconnection at the dayside magnetopause and in the geomagnetic tail, Proc. Intern. Conf. Substorms 1, pp. 117, ESA SP-335, 117–123, 1992.

Elphic, R. C., Means, J. D., Snare, R. C., Strangeway, R. J., Kepko, L., and Ergun,R. E.: Magnetic field instruments for the Fast Auroral Snapshot explorer, Space Sci. Rev. 98, 151–168, 2001.

Escoubet, C. P., Smith, M. F., Fung, S. F., Anderson, P. C., Hoffman,R. A., Basinska, E. M., and Bosqued, J. M.: Staircase ion signature in the polar cusp: A case study, Geophys. Res. Lett., 19, 1735–1738, 1992.

Farrugia, C. J., Southwood, D. J., and Cowley, S. W.: Observations of flux tranfer events, Adv. Space Res., 8(9-10), 249–258, 1988.

Farrugia, C. J., Sandholt, P. E., Cowley, S. W. H., Southwood, D. J., Lepping, R. P., Lazarus, A. J., Egeland, A., Hansen, T., Friis-Christensen, E., and Stauning, P.: Reconnection-associated auroral activity in the presence of two types of upstream dynamic pressure variations: The B_z=0, $B_y \ll 0$ Case, J. Geophys. Res., 100, 21 753–21 772, 1995.

Farrugia, C. J., Sandholt, P. E., Denig, W. F., and Torbert, R. B.: Observation of a correspondence between poleward-moving auroral forms and stepped-cusp ion precipitation, J. Geophys. Res., 103, 9309–9315, 1998.

Farrugia, C. J., Sandholt, P. E., Maynard, N. C., Torbert, R. B., and Ober, D. M.: Temporal variations in a four-sheet field-aligned current system and associated aurorae as observed during a Polar-ground magnetic conjunction at midmorning, J. Geophys. Res., 103 (A6), doi: 10.1029/2002JA009619, 2003.

Farrugia, C. J., Sandholt, P. E., Torbert, R. B., and Ostgaard, N.: Temporal and spatial aspects of the cusp inferred from local and global ground- and space-based observations in a case study, J. Geophys. Res., 109, A04209, doi: 10.1029/2003JA010121, 2004.

Glassmeier, K.-H., and Stellmacher, M.: Mapping flux transfer events to the ionosphere, Adv. Space Res., 18 (8), 151–160, 1996.

Greenwald, R. A.: et al., DARN/SuperDARN: A global view of high-latitude convection, Space Sci. Rev., 71, 763–796, 1995.

Haerendel, G., Paschmann, G., Sckopke, N., Rosenbauer, H., and Hedgecock, P. C.: The frontside boundary layer of the magnetosphere and the problem of reconnection, J. Geophys. Res., 83, 3195–33216, 1978.

Hovestadt, D., Hilchenbach, M., Bürgi, A., et al.: CELIAS–Charge, element, and isotope analysis system for SOHO, Solar Phys., 162, 44–481, 1995.

Kokubun, S, Yamamoto, T., Acuna, M. H., Hayasi, K., Shiokawa, K., and Kawano, H.: The GEOTAIL magnetic field experiment, J. Geomag. Geoelectr., 46, 7–21, 1994.

Lee, L., Kan, J. R., and Akasofu, S.-I.: On the origin of cusp field aligned currents, J. Geophys. Res., 157, 217–221, 1985.

Lockwood, M.: Relationship of dayside auroral precipitations to the open-closed separatrix and the pattern of convective flow, J. Geophys. Res., 102, 17 475–17 487, 1997.

Lockwood, M. and Smith, M. F.: Low-altitude signatures of the cusp and flux transfer events, Geophys. Res. Lett., 16, 879–882, 1989.

Lockwood, M and Smith, M. F.: The variation of reconnection rate at the magnetopause and cusp ion precipitation, J. Geophys. Res., 97, 14 841–14 847, 1992.

Lockwood, M., and Smith, M. F.: Low and middle altitude cusp particle signatures for general magnetopause reconnection rate variations: 1. Theory, J. Geophys. Res., 99, 8531–8553, 1994.

Neudegg, D. A., Yeoman, T. K., Cowley, S. W. H., Provan., G., Haerendel, G., Baumjohann, W., Auster, U., Fornacon, K. H., Georgescu, E., and Owen, C. J.: A flux transfer event observed at the magnetopause by the Equator-S spacecraft and in the ionosphere by the CUTLASS HF radar, Ann. Geophysicae, 17, 707–711, 1999.

Neudegg, D. A., Cowley, S. W. H., Milan, S. E., Yeoman, T. K., Lester, M., Provan, G., Haerendel, G., Baumjohann, W., Nikutowski, B., Buechner, J., Auster, U., Fornacon, K. -H., and Georgescu, E.: A survey of magnetopause FTEs and associated flow bursts in the polar ionopshere, Ann. Geophysicae, 18, 416–435, 2000.

Newell, P. T. and Meng, C.-I.: Ion acceleration at the equatorward edge of the cusp: Low altitude observations of patchy merging, Geophys. Res. Lett., 18, 1829–1832, 1991.

Newell, P. T. and Meng, C.-I.: Mapping the dayside ionosphere to the magnetosphere according to particle precipitation characteristics, Geophys. Res. Lett., 19, 609–612, 1992.

Newell, P. T., Meng, C.-I., Sibeck, D. G., and Lepping, R.: Some

low-altitude cusp dependencies on the interplanetary magnetic field, J. Geophys. Res., 94, 8921–8927, 1989.

Paschmann, G., Haerendel, G., Papamastorakis, I., Sckopke, N., Bame, S. J., Gosling, J. T., and Russell, C. T.: Plasma and magnetic field characteristics of magnetic flux transfer events, J. Geophys. Res., 97, 2159–2168, 1982.

Pinnock, M., Rodger, A. S., Dudeney, J. R., Baker, K. B., Greenwald, R. A., and Greenspan, M.: Observation of an enhanced convection channel in the cusp ionosphere, J. Geophys. Res., 98, 3767–3776, 1993.

Pinnock, M., Rodger, A. S., Dudeney, J. R., Rich, F., and Baker, K. B.: High spatial and temporal resolution observations of the ionospheric cusp, Ann. Geophysicae, 13, 919925, 1995.

Provan, G., Milan, S. E., Lester, M., Yeoman, T. K., and Khan, H.: Simultaneous observations of the ionospheric footprint of flux transfer events and dispersed ion signatures, Ann. Geophysicae, 20, 281–287, 2002.

Reiff, P. and Burch, J. L.: IMF B_y-dependent plasma flow and Birkeland currents in the dayside magnetosphere 2. A global model for northward and southward IMF, J. Geophys. Res., 90, 1595–1609, 1985.

Rème, H., Bosqued, J. M., Sauvaud, J. A. et al.: The CLUSTER ion spectrometry experiment, Space Sci. Rev., 79, 303–350, 1997.

Rijnbeek, R. P. and Cowley, S. W. H.: Magnetospheric flux erosion events are flux transfer events, Nature, 309, 135–138, 1984.

Rodger, A. S. and Pinnock, M.: The ionospheric response to FTEs: the first few minutes, Ann. Geophysicae, 15, 685–691, 1997.

Rosenbauer, H., Grunwaldt, H., Montgomery, M. D., Paschmann, G., and Sckopke, N.: Heos 2 plasma observations in the distant polar magnetosphere: The plasma mantle, J. Geophys. Res., 80, 2723–2737, 1975.

Ruohoniemi, J. M. and Baker, K. B.: Large-scale imaging of high-latitude convection with Super Dual Auroral Radar Network HF radar observations, J. Geophys. Res., 103, 20 797–20 811, 1998.

Russell, C. T. and Elphic, R. C.: Initial ISEE magnetometer results: Magnetopause observations, Space Sci. Rev., 22, 681–715, 1978.

Sandholt, P. E., Deehr, C. S., Egeland, A., Lybekk, B., Viereck, R., and Romick, G. J.: Signatures in the dayside aurora of plasma transfer from the magnetosheath, J. Geophys. Res, 91, 10 063–10 079, 1986.

Sandholt, P. E., Lockwood, M., Oguti, T., Cowley, S. W. H., Freeman, K. S. C., Lybekk, B., Egeland, A., and Willis, D. M.: Midday auroral breakup events and related energy and momentum transfer from the magnetosheath, J. Geophys. Res., 95, 1039–1060, 1990.

Sandholt, P. E., Moen, J., Farrugia, C. J., Cowley, S. W. H., Lester, M., Milan, S., and Denig, W. F., and Eriksson, S.: Multi-site observations of the association between aurora and plasma convection in the cusp/polar cap during a southeast IMF orientation, Ann. Geophysicae, 21, 539, 2003.

Sandholt, P. E., Farrugia, C. J., and Denig, W. F.: Dayside aurora and the role of IMF $|B_y/B_z|$: detailed morphology and response to magnetopause reconnection, Ann. Geophysicae, 22, 613–628, 2004.

Siscoe, G. L. and Cummings, W. D.: On the cause of geomagnetic bays, Planet. and Space Sci., 17, 1795–1802, 1969.

Siscoe, G. L., Lotko, W., and Sonnerup, B. U. O.: A high-latitude, low-latitude boundary layer model of the convection current system, J. Geophys. Res., 96, 3487–3495, 1991.

Smith, C. W., L'Heureux, J., Ness, N. F., Acuña, M. H., Burlaga, L. F., and Scheifele, J.: The ACE magnetic fields experiment, Space Sci. Rev., 86, 613–632, 1998.

Sonnerup, B. U. Ö. and Cahill, L. J.: Magnetopause structure and attitude from explorer 12 observations, J. Geophys. Res., 72, 171–183, 1967.

Sonnerup, B. U. Ö., Paschmann, G., Papamastorakis, I., Sckopke, N., Haerendel, G., Bame, S. J., Asbridge, J. R., Gosling, J. T., and Russell, C. T.: Evidence for reconnection at the earth's magnetopause, J. Geophys. Res., 86, 10 049–10 067, 1981.

Stern, D.: Magnetospheric dynamo processes, in: Magnetospheric Currents, Geophys. Monograph Ser., vol. 28, edited by Potemra, T., AGU, Washington, D.C., 200–207 1984.

Taguchi, S., Sugiura, M., Winningham, J. D., and Slavin, J. A.: Characterization of the IMF B_y-dependent field-aligned currents in the cleft region based on DE 2 observations, J. Geophys. Res., 98, 1393–1407, 1993.

Tanaka, T.: Formation of magnetospheric plasma population regimes coupled with the dynamo process in the convection system, J. Geophys. Res., 108(A8), 1315, doi:10.1029/2002JA009668, 2003.

Thompson, S. M., Kivelson, M. G., Khurana, K. K., Balogh, A., Réme, H., Fazakerley, A. N., and Kistler, L. M.: Cluster observations of quasi-periodic impulisve signatures in the dayside northern lobe: High-latitude flux transfer events, J. Geophys. Res., 109, A02213, doi:10.1029/2003JA010138, 2004.

Trattner, K. J., Fuselier, S. A., Peterson, W. K., Sauvaud, J.-A., Stenuit, H., and Dubouloz, N.: On spatial and temporal structures in the cusp, J. Geophys. Res., 104, 28 411–28 421, 1999.

Trattner, K. J., Fuselier, S. A., Peterson, W. K., Boehm, M., Klumpar, D., Carlson, C. W., and Yeoman, T. K.: Temporal versus spatial interpretation of cusp ion structures observed by two spacecraft, J. Geophys. Res., doi:10.1029/2001JA000181, 2002a.

Trattner, K. J., Fuselier, S. A., Peterson, W. K., Carlson, C. W.: Spatial features observed in the cusp under steady solar wind conditions J. Geophys. Res., 107(A10), doi: 10.1029/2001JA000262, 2002b.

Tsyganenko, N. A.: A magnetospheric magnetic field model with a warped tail plasma sheet, Planet. Space Sci., 37, 4–20, 1989.

Vasyliunas, V. T., Kan, J. R., Siscoe, G. L., and Akasofu, S.-I.: Scaling relations governing magnetospheric energy transfer, Planetary Space Sci., 30, 359–365, 1982.

Watanabe, M., Iijima, T., and Rich, F. J.: Synthesis models of dayside field-aligned currents for strong interplanetary magnetic field B_y, J. Geophys. Res., 101, 13 303–13 319, 1996.

Wild, J. A., Cowley, S. W. H., Davies, J. A., Khan, H., Milan, S. E., Provan, G., Yeoman, T. K., Balogh, A., Dunlop, M. W., Fornacon, K.-H., and Georgescu, E.: First simultaneous observations of flux transfer events at the high-latitude magnetopause by the Cluster spacecraft and pulsed radar signatures in the conjugate ionopsphere by the CUTLASS and EISCAT radars, Ann. Geophysicae, 19, 1491–1508, 2001.

Yeoman, T. K., Lester, M., Cowley, S. W. H., and Milan, S. E.: Simultaneous observations of the cusp in optical, DMSP and HF radar data, Geophys. Res. Lett., 24, 2251–2254, 1997.